Biosensors and Bioelectronics 94 (2017) 19–23

Contents lists available at ScienceDirect

Biosensors and Bioelectronics

journal homepage: www.elsevier.com/locate/bios

Ultrasensitive and selective electrochemical biosensor for detection of mercury (II) ions by nicking endonuclease-assisted target recycling and hybridization chain reaction signal amplification

Minqiang Hong, Mengyan Wang, Jing Wang, Xueqin Xu*, Zhenyu Lin

Ministry of Education Key Laboratory of Analysis and Detection for Food Safety, Fujian Provincial Key Laboratory of Analysis and Detection for Food Safety, College of Chemistry, Fuzhou University, Fuzhou, Fujian 350116, China

ARTICLE INFO

Keywords:
Electrochemical biosensor
Hg^{2+} detection
Nicking endonuclease
Hybridization chain reaction

ABSTRACT

In this paper, a novel and signal-on electrochemical biosensor based on Hg^{2+}- triggered nicking endonuclease-assisted target recycling and hybridization chain reaction (HCR) amplification tactics was developed for sensitive and selective detection of Hg^{2+}. The hairpin-shaped capture probe A (PA) contained a specific sequence which was recognized by nicking endonuclease (NEase). In the presence of Hg^{2+}, probe B (PB) hybridized with PA to form stand-up duplex DNA strands via the Hg^{2+} mediated thymine-Hg^{2+}-thymine (T-Hg^{2+}-T) structure, which automatically triggered NEase to selectively digest duplex region from the recognition sites, spontaneously dissociating PB and Hg^{2+} and leaving the remnant initiators. The released PB and Hg^{2+} could be reused to initiate the next cycle and more initiators were generated. The long nicked double helices were formed through HCR event, which was triggered by the initiators and two hairpin-shaped signal probes labeled with methylene blue, resulting in a significant signal increase. Under optimum conditions, the resultant biosensor showed the high sensitivity and selectivity for the detection of Hg^{2+} in a linear range from 10 pM to 50 nM (R^2=0.9990), and a detection limit as low as 1.6 pM (S/N=3). Moreover, the proposed biosensor was successfully applied in the detection of Hg^{2+} in environment water samples with satisfactory results.

1. Introduction

Mercury is the best-known and most puzzling heavy metal pollutants in the environment (Gochfeld, 2003). It is a causative agent of various sorts of disorders, including neurological, nephrological, immunological, cardiac, reproductive and even genetic (Zahir et al., 2005). The US Environmental Protection Agency (EPA) has set the concentration limit of Hg^{2+} down to 10 nM in drinking water (Wang et al., 2016). Therefore, the sensitive and selective detection of Hg^{2+} in the environment is of great significance.

With the rapid development of contemporary analytical techniques, various methods for detection of Hg^{2+} have been developed, such as high-performance liquid chromatography (HPLC) (Gao and Ma, 2011; Pena-Pereira et al., 2009), atomic absorption spectrometry (AAS) (Kaercher et al., 2005; Madden and Fitzgerald, 2009), cold vapor atomic fluorescence spectrometry (CV-AFS) (Chen et al., 2002; Li et al., 2005), inductively coupled plasma atomic emission spectrometry (ICP-AES) (Han et al., 2006; Zhu and Alexandratos, 2007) and inductively coupled plasma mass spectrometry (ICP-MS) (Gomez-Ariza et al., 2005). However, these instrumental methods are restricted by some defects such as inconvenient, complex sample preparation, expensive apparatus and technical expertise. Thus, there is great need to develop a convenient and rapid detection method for Hg^{2+} analysis.

Electrochemical method is in rapid development in fields of analytical chemistry because of its merits of convenience, excellent sensitivity and good selectivity (Bellin et al., 2016; Tong et al., 2013). It has been proved that Hg^{2+} could be selectively captured by thymine-thymine (T-T) mismatches to form T–Hg^{2+}–T base pairs, which is more stable than adenine-thymine (A-T) pair (Liu et al., 2008; Miyake et al., 2006; Ono and Togashi, 2004). Some electrochemical sensors for Hg^{2+} with excellent performance on selectivity against the interferences of other metal ions have been developed by utilizing the strong T-Hg^{2+}-T interaction (Tang et al., 2014; Yuan et al., 2011; Zhu et al., 2009). On the other hand, many efforts have been put on developing novel electrochemical sensors with high sensitivity. A signal amplification strategy based on nicking endonuclease (NEase) has attracted much attention due to its simple detection process and high selectivity (Hu et al., 2014; Kiesling et al., 2007; Xu et al., 2009). Hybridization chain reaction (HCR) has also been applied in signal amplification strategy in virtue of the property such as excellent amplified signal

* Correspondence to: College of Chemistry, Fuzhou University, Fuzhou, Fujian 350116, China.
E-mail address: xxq@fzu.edu.cn (X. Xu).

http://dx.doi.org/10.1016/j.bios.2017.02.031
Received 16 October 2016; Received in revised form 17 January 2017; Accepted 21 February 2017
Available online 22 February 2017
0956-5663/ © 2017 Elsevier B.V. All rights reserved.

output, simplicity and low-cost (Dong et al., 2012; Peng et al., 2014; Ren et al., 2015). Although the strategy based on NEase-assisted target recycling signal amplification or HCR amplification for electrochemical detection of Hg^{2+} have been reported (Chen et al., 2015; Bao et al., 2015; Li et al., 2016b), the method that combines the above two signal amplification strategy for Hg^{2+} detection has rarely been reported.

In this paper, we report a signal-on electrochemical biosensor for sensitive and selective detection of Hg^{2+} by utilizing NEase-assisted target recycling and HCR for dual signal amplification strategy. A hairpin-shaped capture probe A (PA) contained a specific sequence (5'-GGATC-3'), which was recognized by NEase (Nt.AlWI) and completely blocked in the loop. In the presence of Hg^{2+}, probe B (PB) hybridized with PA to form stand-up duplex DNA strands and provided recognition sites for Nt.AlWI. The initiator sequences were constantly generated with the nicking reaction, PB and Hg^{2+} could then hybridize to another PA and initiate the next cycle of cleavage. The nicked double-helix copolymers were constructed when the two hairpin-shaped signal probes (S_1 and S_2) labeled with methylene blue (MB) were employed to trigger HCR upon the initiator sequences. As a result, the signal was significantly amplified due to the NEase-assisted target recycling and HCR signal amplification strategy. The proposed biosensor could sensitively and selectively detect the ultralow concentration of Hg^{2+}, which was much lower than the EPA limit concentration (10 nM) of Hg^{2+} in drinking water.

2. Material and methods

2.1. Materials

Mercury nitrate standard solution ($Hg(NO_3)_2$, 5.0 mM), Mercaptohexanol (MCH), tris(2-carboxyethyl) phosphine hydrochloride (TCEP) and 2-amino-2- (hydroxymethyl)−1.3-propanediol (Tris) were purchased from Aladdin Chemistry Co., Ltd. (Shanghai, China). The NEase (Nt.AlWI, 10,000 U/mL) and 10×NE buffer 2 (containing 10 mM Tris−HCl, 50 mM NaCl, 10 mM $MgCl_2$ and 1 mM dithiothreitol (DTT), pH 7.9) were purchased from Sangon Biotech Co., Ltd. (Shanghai, China). Tris−HCl buffer 2 (DNA hybridization buffer, pH 8.0) was a mixture of 10 mM Tris−HCl, 100 mM NaCl, 10 mM $MgCl_2$, 10 mM TCEP and 1.0 mM EDTA. Other chemicals were of analytical grade and used without further purification.

All oligonucleotides were synthesized by Sangon Biotech Co., Ltd. (Shanghai, China), and their base sequences in detail were listed as follows:

Hairpin-shaped capture probe A (PA):

5′-HS-$(CH_2)_6$-CCACGGGATCTT TGCAGCGTGG-3′

Probe B (PB): 5′- CTGCTTTGATCC-3′

Hairpin-shaped signal probe one (S_1):

5′-ATGACGGGATCTCACAAAGATCCCGTGG-$(CH_2)_6$-Methylene Blue-3′

Hairpin-shaped signal probe two (S_2):

5′-Methylene Blue-$(CH_2)_6$-TGAGATCCCGTCATCCACGGGAT CTT TG-3′

PA was prepared by dissolving in Tris−HCl buffer 1 containing 10 mM Tris−HCl, 100 mM NaCl, 10 mM $MgCl_2$ and 1.0 mM EDTA (pH 8.0). PB was prepared by dissolving in 1×NE buffer 2. S_1 and S_2 were prepared by dissolving in Tris−HCl buffer 3 containing 20 mM Tris−HCl, 200 mM NaCl and 20 mM $MgCl_2$ (pH 7.4). All the hairpin-shaped oligonucleotides were heated to 90 °C for 5 min and then allowed to cool down to room temperature for 2 h before use. All solutions were prepared with ultrapure water (18.25 MΩ·cm).

2.2. Electrochemical measurements

All electrochemical measurements were performed using a CHI660A electrochemical workstation (shanghai CHI Instruments Co., China). A three-electrode system consisting of the modified gold electrode, an Ag/AgCl reference electrode (saturated KCl) and a platinum wire counter-electrode was used for all the electrochemical measurements. Cyclic voltammetry (CV) were carried out at a scan rate of 0.1 V s^{-1}. Square wave voltammetric (SWV) measurements were performed in 100 mM phosphate buffer solution (PBS, pH7.4, containing 100 mM KCl) with the potential range of 0.1 to −0.5 V, step potential of 4 mV, amplitude of 25 mV, and frequency of 15 Hz. Electrochemical impedance spectroscopy (EIS) measurements were performed in the presence of 5 mM $[Fe(CN)_6]^{4-/3-}$ solution (pH 7.4) containing 100 mM KCl and recorded with the frequency changed from 0.1 Hz to 10 kHz.

2.3. Biosensor preparation and Hg^{2+} detection

The gold electrode (GE, 2 mm in diameter, obtained from Shanghai CHI Instruments Co., China) was polished on alumina (0.05 μm)/water slurry on silk and thoroughly ultrasonicated in ultrapure water, absolute ethanol and ultrapure water for 3 min, respectively. Then the GE was electrochemically cleaned to remove any remaining impurities in 0.5 M H_2SO_4. After drying with nitrogen, the bare GE was immersed in Tris−HCl buffer 1 (containing 1.0 μM PA) in the dark at 37 °C for 3 h, followed by a 2 h treatment with an aqueous solution of 2.0 mM MCH. After that, the modified GE was immersed into the Tris−HCl buffer 2 containing Hg^{2+} of different concentrations, PB and Nt.AlWI for 2 h at 45 °C. Finally, the modified GE was incubated with the mixture of S_1 and S_2 for 100 min at 35 °C. After each step, the electrode was rinsed with PBS (pH7.4) containing 100 mM NaCl to remove the nonspecific adsorption and dried by nitrogen. The modified gold electrode was used for electrochemical measurements.

3. Results and discussion

3.1. Design strategy

The working principle of the dual signal amplification detection strategy is schematically represented in Scheme 1. Hairpin-shaped capture probe A (PA) includes a 5'-GGATC-3' region recognized by Nt.AlWI, and a 14 nucleotide (nt) initiator sequence at the 5′ end. The PA has a stem of 5 base pairs enclosing a 12 nt loop and cannot be cut by Nt.AlWI in the absence of Hg^{2+}. With the presence of Hg^{2+}, PA hybridized with PB to form stand-up duplex DNA strands via the Hg^{2+} mediated with T−Hg^{2+}−T base pairs, which automatically triggered Nt.AlWI to selectively digest duplex region from the recognition sites, spontaneously dissociating PB and Hg^{2+}, and leaving the remnant initiators. The released PB and Hg^{2+} could be reused to initiate the next cycle, resulting in an increasing number of initiators. These initiators were able to hybridize with S_1 and trigger the HCR event. The continued hybridization of S_1 and S_2 led to successful HCR process that formed nicked double helices, resulting in a significant increase of the current signal of MB. As a result, the signal was significantly amplified due to the NEase-assisted target recycling and HCR signal amplification strategy.

3.2. Feasibility testing of the biosensor

The feasibility of the proposed electrochemical biosensor for Hg^{2+} detection was firstly investigated by SWV. The typical SWV responses of the reduction reaction of MB tagged on signal probes (S_1/S_2) at different experimental stages were revealed in Fig. 1A. Before Hg^{2+} was introduced, only a teeny reduction current was observed (14.2 nA, curve a) when S_1 was added to the HCR process, probably resulted from the nonspecific adsorption of S_1. Otherwise, without S_1, there was a small reduction current (16.2 nA, curve b) when S_2 was added to the HCR process, even in the presence of Hg^{2+}. In the absence of Hg^{2+}, a small reduction current was observed (42.0 nA, curve c) as S_1 and S_2 were added to the HCR process, which was probably attributed to

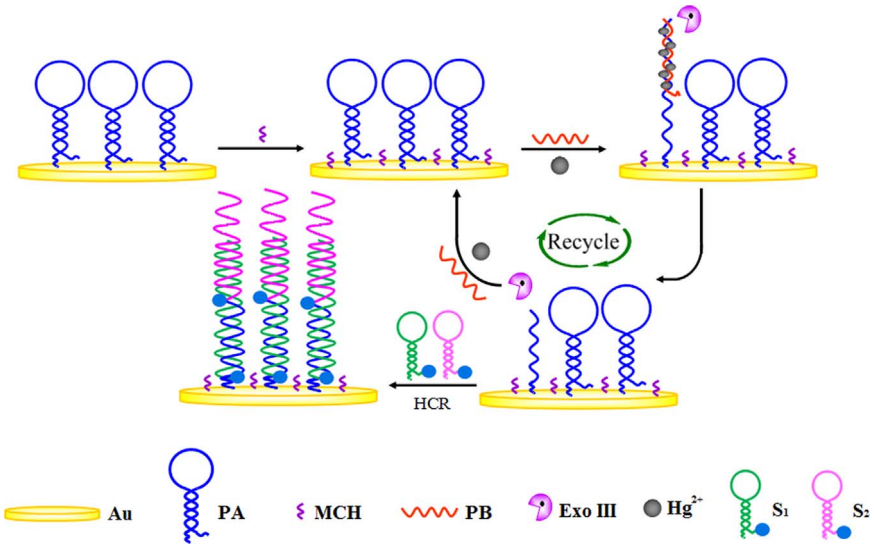

Scheme 1. Schematic diagram of electrochemical sensor for the detection of Hg^{2+} based on NEase assisted Hg^{2+} recycling and HCR amplification strategy.

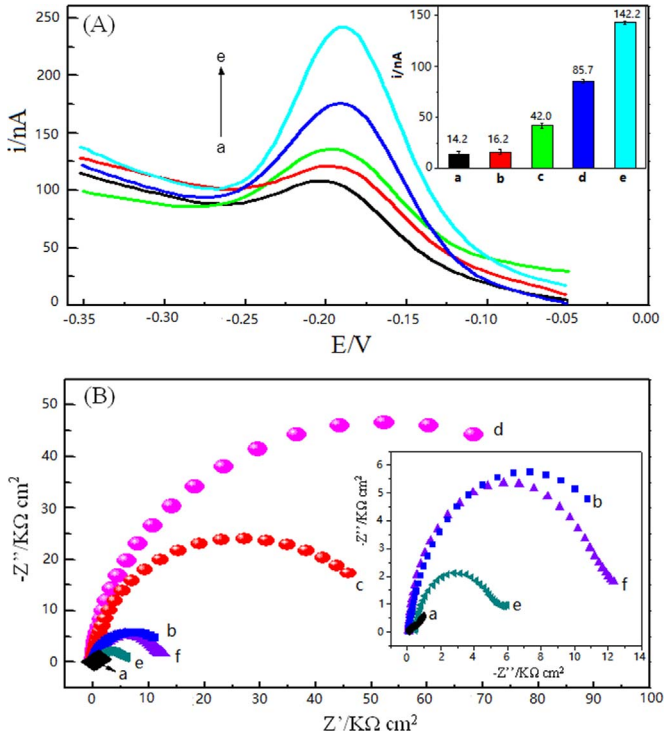

Fig. 1. (A) Typical SWV responses of system under different conditions: (a) PA+MCH +PB+Nt.AlWI+S_1, (b) PA+MCH+PB+Hg^{2+}+Nt.AlWI+S_2, (c) PA+MCH+PB+Nt.AlWI +S_1+S_2, (d) PA+MCH+PB+Hg^{2+}+Nt.AlWI+S_1, (e) PA+MCH+PB+ Hg^{2+}+Nt.AlWI +S_1+S_2. Concentrations: PA (1.0 μM), PB (0.2 μM), Nt.AlWI (0.20 U/μL), MCH (2 mM), Hg^{2+}(25 nM), S_1 (2.0 μM) and S_2 (2.0 μM). Inset: Column diagram of resulting peak currents for different strategies. The illustrated error bars represented the standard deviations of three parallel experiments (the same below). (B) Electrochemical impedance spectra (EIS) of the progressively modified step of biosensor in 5 mM $[Fe(CN)_6]^{3-/4-}$ containing 0.1 M KCl: (a) bare GE, (b) PA/GE, (c) MCH/PA/GE, (d) c incubated with 0.2 μM PB containing 5.0 nM Hg^{2+}, (e) d incubated with 0.20 U/μL Nt.ALWI, (f) e incubated with 2.0 μM S_1 and 2.0 μM S_2. Inset: Drawing of partial enlargement.

nonspecific adsorption of small amount of signal probes. As the result of single HCR amplification, curve d showed a 6-fold electrochemical signal (85.7 nA) for NEase-assisted signal amplification. Furthermore, a 10-fold peak current was observed (142.2 nA, curve e) for NEase-assisted signal amplification and HCR signal amplification strategy, revealing an efficient and excellent dual signal amplification capability of the resultant biosensor.

3.3. Electrochemical characterizations of the biosensor

The changes of electron transfer resistance (R_{et}) could reflect the different modification processes that occur on the electrode surface. As shown in Fig. 1B, the pretreated bare GE had a relatively low impedance with a small semicircle domain (curve a), indicating excellent electrochemical conductivity of the treated GE. After PA was assembled consecutively onto the GE, the R_{et} increased apparently (curve b) as the increasing oligonucleotides on the GE hindered the electron-transfer. The R_{et} kept increasing (curve c) when the GE was blocked unoccupied sites by MCH. After PB and Hg^{2+} were also assembled on the electrode, the R_{et} further increased (curve d), indicating that PA hybridized with PB via T–Hg^{2+}–T structure. A sharply decreased semicircle domain (curve e) was observed after incubating with Nt.AlWI, which was owed to the nicking reaction. Subsequently, a larger semicircle domain was observed (curve f) when the hybridization between the initiators and two signal probes (S_1 and S_2) occurred for HCR signal amplification strategy. The above changes of electron transfer resistance show that the biosensor is of good feasibility.

3.4. Optimization of assay conditions

In order to obtain optimum analytical parameters, both concentration of Nt.AlWI and incubation temperature were optimized. SWV was used to monitor the current signal change (Δi) (Δi=i_1–i_2, where i_1 and i_2 are the reduction peak current of MB tags in the presence and absence of Hg^{2+}, respectively). As shown in Fig. 2A, the Δi increased remarkably till Nt.AlWI concentration increased to 0.20 U/μL. Then, the Δi slowly decreased with increasing Nt.AlWI concentration from 0.20 U/μL to 0.30 U/μL, which was mostly due to the fact that the amount of the generated initiators reached the maximum when the Nt.AlWI concentration was 0.2 U/μL. The results indicated that the optimum concentration of Nt.AlWI was 0.20 U/μL. The Δi increased remarkably till the temperature increased to 45 °C, but decreased as the temperature beyond 45 °C (see Fig. 2B), which was attributed to the fact that Nt.AlWI reached the maximum activity when the temperature was 45 °C. Therefore, 45 °C was used as the optimal incubation temperature.

The hybridization chain reaction time and the concentration of S_1 and S_2 during the HCR course were also optimized. As the time increased to 100 min, the Δi trended to a plateau since the HCR was

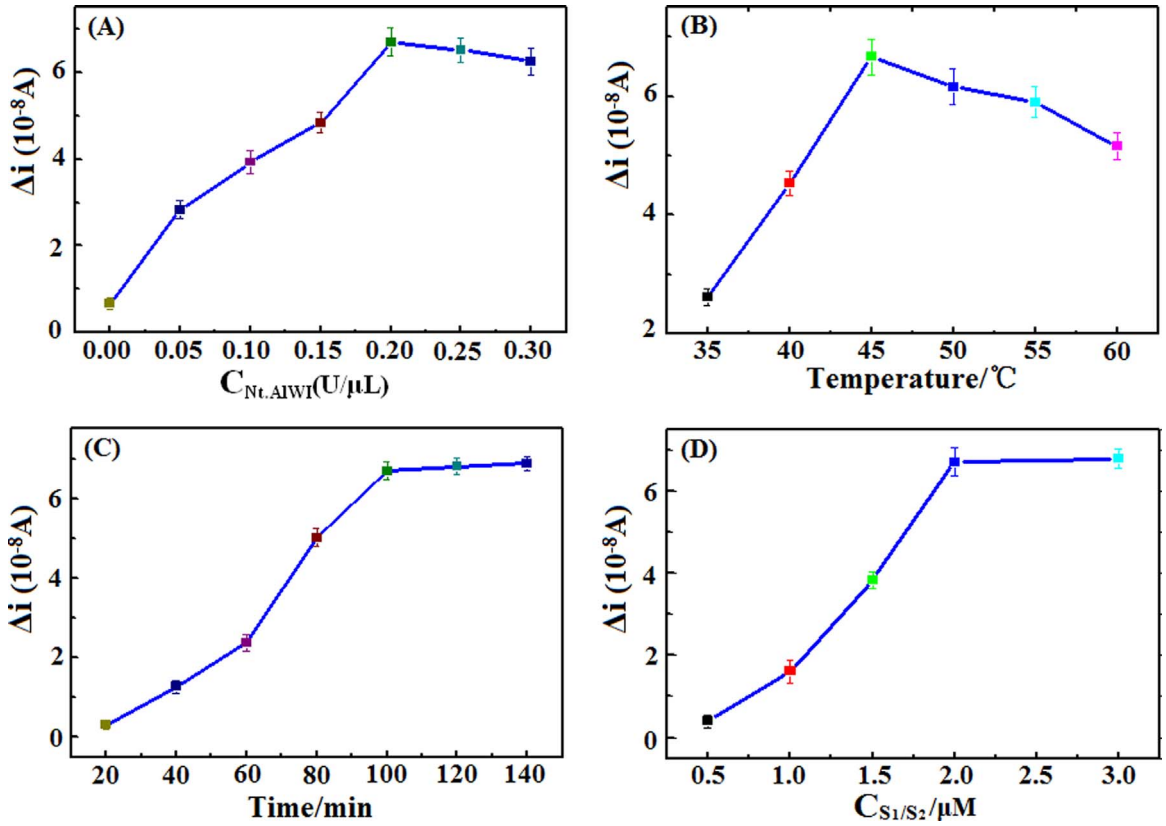

Fig. 2. (A) Effect of different concentration of Nt.AlWI in the presence of 5.0 nM Hg^{2+}. (B) Effect of incubation temperature in the presence of 5.0 nM Hg^{2+}. (C) Effect of hybridization chain reaction time in the presence of 5.0 nM Hg^{2+}. (D) Effect of the concentration of S_1 and S_2 in the presence of 5.0 nM Hg^{2+}.

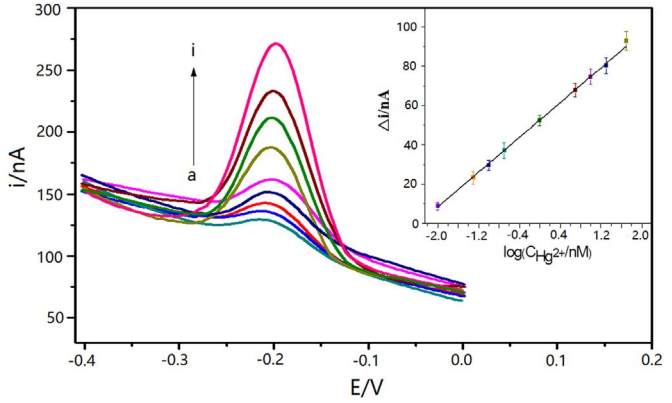

Fig. 3. SWV responses for the detection of different concentrations of Hg^{2+}. From bottom to top (a–i): 0.01 nM, 0.05 nM, 0.1 nM, 0.2 nM, 1.0 nM, 5.0 nM, 10 nM, 20 nM, 50 nM. Inset: Linear relationship between the current signal change (Δi) and the logarithm of the concentration of Hg^{2+}.

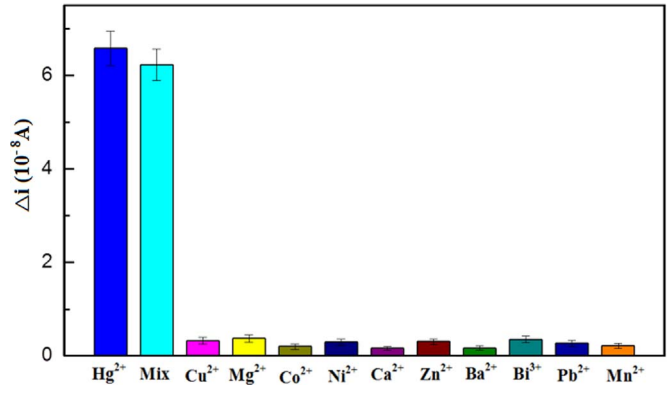

Fig. 4. Selectivity of the biosensor for Hg^{2+}(5.0 nM), several competing 10 interfering metal ions (Cu^{2+}, Mg^{2+}, Co^{2+}, Ni^{2+}, Ca^{2+}, Zn^{2+}, Ba^{2+}, Bi^{3+}, Pb^{2+}, Mn^{2+}) (1.0 μM) and a mixture (Mix) of the interference metal ions (1.0 μM) and Hg^{2+}(5.0 nM) in the presence of Nt.AlWI (0.20 U/μL), MCH (2 mM), probe A (1.0 μM), probe B (0.2 μM), S_1 (2.0 μM) and S_2 (2.0 μM).

almost completed when the time was 100 min (see Fig. 2C). Thus, 100 min was selected as the optimum hybridization chain reaction time. In addition, the Δi increased significantly till the concentration of S_1 and S_2 increased to 2.0 μM (see Fig. 2D), probably owing to the distant-sensitive electrochemical reaction. Therefore, the optimal concentration of S_1 and S_2 was chosen as 2.0 μM.

3.5. Sensitivity of the biosensor

Under optimum conditions, the sensitivity of the electrochemical biosensor for the detection of the Hg^{2+} was investigated by varying the Hg^{2+} concentrations. It was obviously observed that the current signal of MB tag increased with the increasing of Hg^{2+} concentrations (see Fig. 3). The plot of the current signal change (Δi) vs. the logarithm of

Table 1
Determination of Hg^{2+} in Environmental Water Samples.

Sample	Added (nM)	Found (nM)	Recovery (%)	RSD (%, n=3)
Tap water 1	0	a		
Tap water 2	1.0	0.97	97.0	5.2
Tap water 3	5.0	4.86	97.2	5.0
Lake water 1	0	a		
Lake water 2	5.0	5.15	103	4.3
Lake water 3	10.0	9.67	96.7	4.9

a: No Hg^{2+} was detected.

Hg^{2+} concentration showed a linear relationship in the detection range from 10 pM to 50 nM with a sensitivity of 22.1 nA per decade (inset in Fig. 3). The regression equation was $\Delta i/nA=52.57+22.1 \log (C_{Hg2+}/nM)$ ($R^2=0.9990$), where Δi is SWV current increment, the C_{Hg2+} is the concentration of Hg^{2+}, R^2 is regression coefficient. The detection limit (DL) was calculated to be 1.6 pM at a signal to noise ratio of 3, which was much lower than that of the other electrochemical biosensors for Hg^{2+} based on single NEase amplification (Chen et al., 2015), HCR amplification (Li et al., 2016b) or gold nanoparticle amplification (Zhu et al., 2009). Compared to the existing Hg^{2+} sensors by the fluorescent method (Gao et al., 2016; Lv et al., 2016; Ma et al., 2013) and colorimetric method (Li et al., 2016a), this electrochemical Hg^{2+} biosensor showed higher sensitivity due to the NEase-assisted target recycling and HCR signal amplification strategy.

3.6. Selectivity and reproducibility of the biosensor

Previous studies have demonstrated that thymine-thymine (T-T) mismatches have a high specificity in distinguishing the target Hg^{2+} from other metal ions. The effects of 10 interfering ions (Cu^{2+}, Mg^{2+}, Co^{2+}, Ni^{2+}, Ca^{2+}, Zn^{2+}, Ba^{2+}, Bi^{3+}, Pb^{2+}, Mn^{2+}) and the mixture (Mix) (consisted of the 10 interference metal ions (1.0 μM) and 5.0 nM Hg^{2+}) on the biosensor were investigated, respectively. As shown in Fig. 4, it was obviously observed that the Δi was not increased remarkably with the addition of a number of metal ions at a concentration which was 200-fold of the Hg^{2+} concentration in the absence of Hg^{2+}. These results showed that the proposed sensor had high selectivity.

The reproducibility of the biosensor was investigated by monitoring the current signal in the presence of 0.5 nM Hg^{2+} for 10 replicate determinations under the same conditions. The relative standard deviation (RSD) of the biosensor was found to be 4.8%, demonstrating its good reproducibility.

3.7. Application to environment water samples

We attempted to evaluate the practical application of the electrochemical biosensor by determining the recovery of added Hg^{2+} in tap water samples and lake water samples. At first, all the collected samples were filtered through 0.22 μm membranes to remove the insoluble impurities and diluted with nitric acid (1 M) at a volume ratio of 1:1, afterwards, Hg^{2+} stock solution at different concentrations was added in these samples, and the biosensor was then employed to detect Hg^{2+} concentration. The results are summarized in Table 1, the recovery values were between 96.7% and 103%, illustrating the favorable potential of the biosensor to be applied in real samples.

4. Conclusions

In summary, a novel and signal-on electrochemical biosensor based on NEase-assisted target recycling and HCR signal amplification strategy has been designed for the detection of Hg^{2+}. With the aid of the dual signal amplification strategy, the proposed biosensor exhibits high sensitivity with the detection limit of 1.6 pM. More importantly, the signal-on mechanism can efficiently avoid false positive results. Moreover, the resultant biosensor can discriminate Hg^{2+} from other metal ions with high selectivity. The proposed biosensor not only can be used for the routine detection of Hg^{2+} in water, but also has a great potential for applications in the detection of ultratrace Hg^{2+} in other complex samples.

Acknowledgments

This work was supported by the National Natural Science Foundation of China (21475024) and the Program for Changjiang Scholars and Innovative Research Team in University (No. IRT_15R11), China.

References

Bao, T., Wen, W., Zhang, X.H., Xia, Q.H., Wang, S.F., 2015. Biosens. Bioelectron. 70, 318–323.
Bellin, D.L., Sakhtah, H., Zhang, Y.H., Price-Whelan, A., Dietrich, L.E.P., Shepard, K.L., 2016. Nat. Commun. 7, 10535.
Chen, D.M., Gao, Z.F., Jia, J., Li, N.B., Luo, H.Q., 2015. Sens. Actuators B-Chem. 210, 290–296.
Chen, Y.W., Tong, J., D'Ulivo, A., Belzile, N., 2002. Analyst 127, 1541–1546.
Dong, J., Cui, X., Deng, Y., Tang, Z., 2012. Biosens. Bioelectron. 38, 258–263.
Gao, Z.B., Ma, X.G., 2011. Anal. Chim. Acta 702, 50–55.
Gao, Z.H., Lin, Z.Z., Chen, X.M., Lai, Z.Z., Huang, Z.Y., 2016. Sens. Actuators B-Chem. 222, 965–971.
Gochfeld, M., 2003. Ecotoxicol. Environ. Saf. 56, 174–179.
Gomez-Ariza, J.L., Lorenzo, F., Garcia-Barrera, T., 2005. Anal. Bioanal. Chem. 382, 485–492.
Han, F.X., Patterson, W.D., Xia, Y.J., Sridhar, B.B.M., Su, Y., 2006. Water Air Soil Pollut. 170, 161–171.
Hu, Y.H., Xu, X.Q., Liu, Q.H., Wang, L., Lin, Z.Y., Chen, G.N., 2014. Anal. Chem. 86, 8785–8790.
Kaercher, L.E., Goldschmidt, F., Paniz, J.N.G., de Moraes Flores, É.M., Dressler, V.L., 2005. Spectrochim. Acta B 60, 705–710.
Kiesling, T., Cox, K., Davidson, E.A., Dretchen, K., Grater, G., Hibbard, S., Lasken, R.S., Leshin, J., Skowronski, E., Danielsen, M., 2007. Nucleic Acids Res. 35, e117.
Li, S.P., Lai, J.P., Qi, L.M., Saqib, M., Majeed, S., Tong, Y.J., Xu, G.B., 2016a. Analyst 141, 2362–2366.
Li, Z.B., Miao, X.M., Xing, K., Peng, X., Zhu, A.H., Ling, L.S., 2016b. Biosens. Bioelectron. 80, 339–343.
Li, Y., Yan, X.P., Dong, L.M., Wang, S.W., Jiang, Y., Jiang, D.Q., 2005. J. Anal. At. Spectrom. 20, 467–472.
Liu, C.W., Hsieh, Y.T., Huang, C.C., Lin, Z.H., Chang, H.T., 2008. Chem. Commun. 19, 2242–2244.
Lv, X.X., Wu, W.C., Niu, C.G., Huang, D.W., Wang, X.Y., Zhang, X.G., 2016. Talanta 151, 62–67.
Ma, J., Chen, Y.H., Hou, Z., Jiang, W., Wang, L., 2013. Biosens. Bioelectron. 43, 84–87.
Madden, J.T., Fitzgerald, N., 2009. Spectrochim. Acta B 64, 925–927.
Miyake, Y., Togashi, H., Tashiro, M., Yamaguchi, H., Oda, S., Kudo, M., Tanaka, Y., Kondo, Y., Sawa, R., Fujimoto, T., 2006. J. Am. Chem. Soc. 128, 2172–2173.
Ono, A., Togashi, H., 2004. Angew. Chem. 43, 4300–4302.
Pena-Pereira, F., Lavilla, I., Bendicho, C., Vidal, L., Canals, A., 2009. Talanta 78, 537–541.
Peng, K., Zhao, H.W., Yuan, Y.L., Yuan, R., Wu, X.F., 2014. Biosens. Bioelectron. 55, 366–371.
Ren, W., Gao, Z.F., Li, N.B., Luo, H.Q., 2015. Biosens. Bioelectron. 63, 153–158.
Tang, S.R., Tong, P., Lu, W., Chen, J.F., Yan, Z.M., Zhang, L., 2014. Biosens. Bioelectron. 59, 1–5.
Tong, Y.J., Li, H.D., Guan, H.M., Zhao, J.M., Majeed, S., Anjum, S., Liang, F., Xu, G.B., 2013. Biosens. Bioelectron. 47, 553–558.
Wang, H., Zhang, Y.H., Ma, H.M., Ren, X., Wang, Y.G., Zhang, Y., Wei, Q., 2016. Biosens. Bioelectron. 86, 907–912.
Xu, W., Xue, X.J., Li, T.H., Zeng, H.Q., Liu, X.G., 2009. Angew. Chem. Int. Ed. 48, 6849–6852.
Yuan, T., Liu, Z.Y., Hu, L.Z., Zhang, L., Xu, G.B., 2011. Chem. Commun. 47, 11951–11953.
Zahir, F., Rizwi, S.J., Haq, S.K., Khan, R.H., 2005. Environ. Toxicol. Pharmacol. 20, 351–360.
Zhu, X.P., Alexandratos, S.D., 2007. Microchem. J. 86, 37–41.
Zhu, Z.Q., Su, Y.Y., Li, J., Li, D., Zhang, J., Song, S.P., Zhao, Y., Li, G.X., Fan, C.H., 2009. Anal. Chem. 81, 7660–7666.